Journal of Advances in Mathematics and Computer Science

xx(x): ....., 20yy; Article no.JAMCS.xxxxx

ISSN: 2456-9968

(Past name: British Journal of Mathematics & Computer Science, Past ISSN: 2231-0851)

Mathematical Model for the Population Dynamics of *Aedes aegypti* Under Extreme Temperature Conditions

Original Research Article

Received: XX December 20XX
Accepted: XX December 20XX
Online Ready: XX December 20XX

Abstract

Aims/ objectives: To develop and analyze a mathematical model for the population dynamics of *Aedes aegypti* under extreme temperature conditions, focusing on endemic and non-endemic regions of Salta, Argentina.
Study design: Deterministic mathematical modeling study.
Place and Duration of Study: Faculty of Natural Sciences and Faculty of Exact Sciences, National University of Salta, Argentina; simulations and analysis conducted during the research period 2025.
Methodology: Building upon the differential equation framework proposed by Yang et al., entomological parameters were redefined using piecewise continuous functions to extend validity beyond the $10 - 40\,^{\circ}\mathrm{C}$ experimental range. This extension is supported by empirical evidence at extreme temperatures, consistent with laboratory observations, thereby ensuring the biological plausibility of the model. The model incorporates larval, pupal, and adult stages. Equilibrium points and stability were analyzed through the Routh–Hurwitz criteria. A local sensitivity analysis of the temperature-dependent basic offspring number $Q_0^*(T)$ was conducted. This indicator estimates the average number of female mosquitoes produced by a single female at a given temperature after surviving the immature stages, and it differs from the classical basic reproduction number R_0, which quantifies the average number of infectious individuals generated in fully susceptible populations. Numerical simulations were performed for three contrasting departments (Orán, Capital, La Poma).
Results: The analysis shows that mosquito persistence or extinction is strongly conditioned by temperature through $Q_0^*(T)$. Parameters such as oviposition rate, larval survival, and the proportions of larvae and female adults (k and f) are the most influential. Simulations reproduce local patterns: persistence in warmer regions (Orán, Capital) and extinction in colder regions (La Poma), consistent with field data.
Conclusion: The extended model ensures mathematical consistency under extreme temperatures and provides a consistent framework for predicting vector dynamics in diverse climatic scenarios. These findings strengthen the link between theoretical modeling and empirical evidence, offering relevant implications for public health strategies against dengue in northern Argentina.

Keywords: Aedes, dengue, temperature, modeling, stability, sensitivity.

2010 Mathematics Subject Classification: 53C25; 83C05; 57N16

1 Introduction

Dengue is a viral disease transmitted through the bite of the *Aedes aegypti* mosquito, which has affected the province of Salta, Argentina, for more than 20 years (National Directorate of Epidemiology and Health Situation Analysis, 2021; Avilés, 2000; Chanampa, 2019). Understanding aspects of the vector's population dynamics, based on estimates of local parameters, is of great importance.
If the disease is not controlled through mosquito eradication, more pronounced outbreaks could occur in the coming years, potentially overwhelming the resources of the provincial health system. For instance, in 2023 Argentina registered 16,143 cases of dengue up to week 12. This number represents a significant increase compared to the last two years, although it is still 10% lower than in 2020 and 40% lower than in 2016, two previous epidemic seasons (General Directorate of Epidemiological Coordination, 2023).
In this epidemiological context, it is crucial to analyze the problem from a mathematical perspective, with the aim of understanding and predicting key aspects of disease spread. Dengue can be modeled, numerically simulated, and described in regional scenarios, investigating the influence of temperature in different areas of the province on the mosquito's life cycle. Yang et al. (2009, 2011) conducted laboratory experiments and showed that at low temperatures there is no development of immature forms into adults nor an increase in oviposition; while at high temperatures, only the development of immature forms is observed. Their results are based on a temperature range between $10\,^{\circ}\mathrm{C}$ and $40\,^{\circ}\mathrm{C}$. These findings coincide with references from the Ministry of Public Health of Argentina. For example, *Aedes aegypti* larvae cannot withstand temperatures below $10\,^{\circ}\mathrm{C}$ or above $45\,^{\circ}\mathrm{C}$; furthermore, below $13\,^{\circ}\mathrm{C}$ the transition to the pupal stage is interrupted.
Moreover, Bar-Zeev (1958) reported that the developmental threshold is between 9 and $10\,^{\circ}\mathrm{C}$, and demonstrated that the maximum and minimum temperatures enabling development from newly hatched larvae to adult are $36\,^{\circ}\mathrm{C}$ and $14\,^{\circ}\mathrm{C}$, respectively. These entomological parameters, extensively referenced in the scientific literature, are consistent with the ranges documented in Argentina.
In addition, Focks et al. (1993), through the validation of the CIMSiM model, analyzed the critical transition in the development of *Aedes aegypti* larvae when moving from resource scarcity to food abundance. Laboratory experiments established that food availability limits growth only up to a threshold of approximately 600 mg per container; below this threshold, larval development is slow and mortality is high, whereas above it survival and development rates become independent of food density, with temperature emerging as the sole determinant of maturation speed. This finding reinforces the conclusion that temperature is the dominant ecological factor governing mosquito development once nutritional constraints are overcome.
Taken together, these experimental findings highlight the central role of temperature in mosquito development. Since it is difficult to replicate these experiments in a laboratory, the mathematical results on survival rates are adapted to understand what happens in regions of interest in Salta. The city of Marília, in the state of São Paulo, Brazil, from which these rates were experimentally derived, lies within the same geographic region as the departments of Orán, Capital, and La Poma, in the province of Salta, Argentina. All of these locations are situated in the Southern Hemisphere and share similar subtropical and tropical climatic conditions, as they are aligned along a latitude close to the Tropic of Capricorn. Considering background information on the presence or absence of *Aedes aegypti* in Salta, entomological parameters were determined for Orán, Capital, and La Poma, departments located in different ecoregions and exhibiting contrasting climatic conditions.
La Poma was chosen to compare findings reported in the literature with results obtained through simulations under different modeled scenarios. This comparison allows for exploring the model's limitations in contexts unfavorable for the presence of the vector. Moreover, it is important to extend these analyses to colder climates, since previous studies have indicated that expansion into such environments is possible (Alonso et al., 2022). Understanding the dynamics in cold regions is therefore essential to anticipate potential shifts in the distribution of *Aedes aegypti*.
Orán was also included due to the abundance of data and studies on the strong presence of *Aedes*

aegypti, and Capital due to its history of dengue transmission under climatic conditions different from those of Orán. In total, three departments were selected that exhibit marked contrasts in temperature, vector presence, and disease prevalence. Since the regions of interest experience average annual temperatures below $10\,^{\circ}\mathrm{C}$, it is necessary to extend the temperature range considered in the model. To this end, a redefinition of entomological parameters using piecewise continuous functions is proposed. Yang et al. (2011) proposed a mathematical model of differential equations that describes the mosquito population dynamics, determining equilibrium points and their local stability. However, this work did not address sensitivity or bifurcation analysis. The objective of this article is to expand the study of the model by considering a redefinition of the entomological parameters, upon which all subsequent analyses are based. In particular, the stability analysis of the equilibria, the sensitivity analysis of parameters, and numerical simulations are addressed, with results compared to fieldwork carried out in Salta.

2 Materials and Methods

2.1 Entomological Parameters and Temperature Dependence

The mathematical framework used to define the entomological parameters of the model is based on the polynomial equation proposed by Yang et al. (2009, 2011). This equation describes biological rates in units of day^{-1} as a function of temperature T.
The parameters considered and their dependence on temperature T are:

- $\phi(T)$: *Per capita* oviposition rate.
- $\mu_l(T)$: Larval mortality rate.
- $\pi_l(T)$: Transition rate from larva to pupa.
- $\mu_p(T)$: Pupal mortality rate.
- $\pi_p(T)$: Transition rate from pupa to adult.
- $\mu_f(T)$: Adult mosquito mortality rate.

The polynomial coefficients (b_n) and the temperature validity ranges for each parameter are presented in Table 1.
To ensure continuity of the function and to avoid mathematical inconsistencies (such as division by zero) in subsequent simulations outside the validity ranges, each parameter is redefined using the asterisk notation (for example, $\phi^*(T)$). This extension incorporates the image of the extreme values. In particular, the following estimates for a mean temperature of $6.5^{\circ}\mathrm{C}$ illustrate the consistency of the redefined parameters:

- The oviposition rate, ϕ^*, is 1.6×10^{-4}, indicating that daily egg-laying is practically null.
- Larval mortality, μ_l^*, reaches 18% per day, implying an average lifespan of five days.
- Pupal mortality, μ_p^*, is approximately 17% per day, with a similar average lifespan of five days.
- Adult female mortality, μ_f^*, is 18% per day, again corresponding to an average lifespan of five days.
- Only 1.9×10^{-5}% of individuals complete the transition from larva to pupa, π_l^*, with a larval period of 52 days.
- Barely 1.5×10^{-6}% succeed in completing the transition from pupa to adult, π_p^*, with a pupal period of 666 days.

These values coincide with the laboratory observations reported by Yang and colleagues, who demonstrated that at low temperatures immature forms do not develop into adults and oviposition does not increase. This experimental concordance reinforces the validity of the defined parameters and

their relevance for modeling local scenarios. Thus, the rates are redefined by the following piecewise functions, as illustrated in Figure 1.

Table 1: Estimated coefficients for the polynomial fitting of entomological parameters as a function of temperature T (in $10\,^{\circ}\mathrm{C}$).

Coefficients	$\phi(T)$	$\mu_l(T)$	$\mu_p(T)$	$\mu_f(T)$	$\pi_l(T)$	$\pi_p(T)$
b_0	-5.400	2.315	4.256×10^{-1}	8.692×10^{-1}	-1.847	5.397×10
b_1	1.800	-4.191	-3.248×10^{-2}	-1.590×10^{-1}	8.291×10^{-1}	-2.321×10
b_2	-2.124×10^{-1}	-2.735×10^{-2}	7.060×10^{-4}	1.116×10^{-2}	-1.457×10^{-1}	4.212
b_3	1.015×10^{-2}	-7.538×10^{-4}	4.395×10^{-7}	-3.408×10^{-4}	1.304×10^{-2}	4.213×10^{-1}
b_4	-1.515×10^{-4}	7.503×10^{-6}		3.809×10^{-6}	-6.461×10^{-4}	2.545×10^{-2}
b_5					1.796×10^{-5}	-9.506×10^{-4}
b_6					-2.617×10^{-7}	2.146×10^{-5}
b_7					1.551×10^{-9}	-2.681×10^{-7}
b_8						1.420×10^{-9}
Range $[T_{\min} - T_{\max}]$	$[11.63 - 37.20]$	$[10 - 40]$	$[10 - 40]$	$[10 - 40]$	$[11.96 - 40.55]$	$[10.31 - 40.08]$

$$
\begin{aligned}
\phi^*(T) &= \begin{cases} \phi(11.63) & \text{if } T \le 11.63 \\ \phi(T) & \text{if } 11.63 < T < 37.20 \\ \phi(37.20) & \text{if } T \ge 37.20 \end{cases} \qquad
\mu_l^*(T) = \begin{cases} \mu_l(10) & \text{if } T \le 10 \\ \mu_l(T) & \text{if } 10 < T < 40 \\ \mu_l(40) & \text{if } T \ge 40 \end{cases} \\
\mu_p^*(T) &= \begin{cases} \mu_p(10) & \text{if } T \le 10 \\ \mu_p(T) & \text{if } 10 < T < 40 \\ \mu_p(40) & \text{if } T \ge 40 \end{cases} \qquad
\mu_f^*(T) = \begin{cases} \mu_f(10) & \text{if } T \le 10 \\ \mu_f(T) & \text{if } 10 < T < 40 \\ \mu_f(40) & \text{if } T \ge 40 \end{cases} \\
\pi_l^*(T) &= \begin{cases} \pi_l(11.96) & \text{if } T \le 11.96 \\ \pi_l(T) & \text{if } 11.96 < T < 40.55 \\ \pi_l(40.55) & \text{if } T \ge 40.55 \end{cases} \qquad
\pi_p^*(T) = \begin{cases} \pi_p(10.31) & \text{if } T \le 10.31 \\ \pi_p(T) & \text{if } 10.31 < T < 40.08 \\ \pi_p(40.08) & \text{if } T \ge 40.08 \end{cases}
\end{aligned} \tag{2.1}
$$

2.2 Population Dynamics Model

The population dynamics of *Aedes aegypti* are modeled based on its life cycle, composed of three stages: two aquatic phases (larva L and pupa P) and one adult phase (mosquitoes M) (Yang et al., 2011). The model proposed by Yang et al. (2011) adopts a compartmental structure of ordinary differential equations (ODEs), a methodology that has been recently classified and validated in the systematic review by San Miguel et al. (2024). This review emphasizes that such deterministic models are crucial for understanding how environmental factors, particularly temperature, affect the mosquito's life cycle.

The dynamics proposed by Yang *et al.* for the mosquito life cycle are based on the assumption that the number of larvae L at time t is determined by the increase due to eggs deposited by females that hatch, and decreases according to the transition rate from larvae to pupae $\pi_l^*(T)$ and the larval mortality rate $\mu_l^*(T)$. The number of eggs φ is defined as $\varphi(M) = \phi^* M$, where ϕ^* denotes the per capita oviposition rate and M represents the number of female mosquitoes.

The expression $M\left(1 - \frac{L}{C}\right)$ represents the effective rate of larval production, where $\left(1 - \frac{L}{C}\right)$ corresponds to the available container capacity to receive larvae from hatched eggs, with C denoting the total carrying capacity of the containers.

Similarly, the number of pupae P at time t increases due to the transition from larvae to pupae, $\pi_l^*(T)$, and decreases through the transformation of pupae into adult mosquitoes and pupal mortality, $\pi_p^*(T)$ and $\mu_p^*(T)$, respectively.

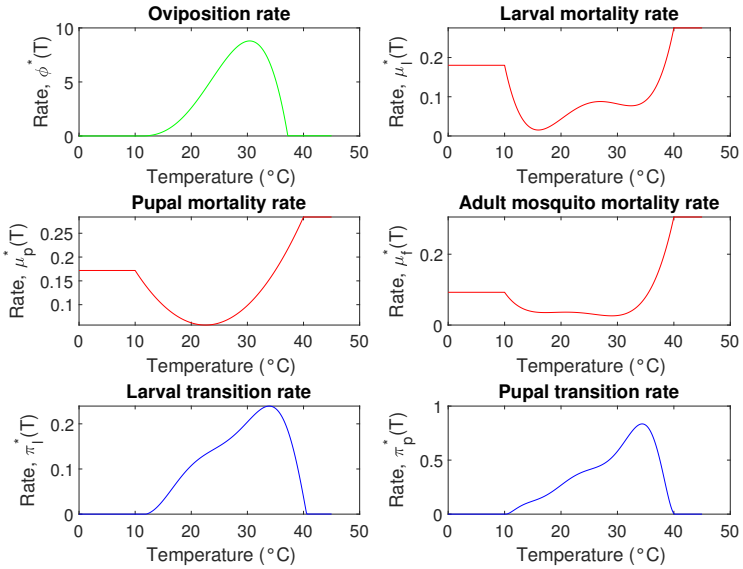

Figure 1: Entomological parameters ϕ^*, μ_l^*, μ_p^*, μ_f^*, π_l^* and π_p^* as a function of temperature in degrees Celsius, for $T \in [0, 45]$.

Finally, the number of female mosquitoes M at time t increases with the emergence of pupae, $\pi_p^*(T)$, and decreases according to the adult female mortality rate $\mu_f^*(T)$.
The model incorporates essential assumptions for population dynamics, such as the sufficient availability of males for mating (Eiman et al., 2010). In addition, it includes three input parameters whose values will be defined in the simulation section:

- The carrying capacity (C) of breeding sites, understood as a standardized reproduction site (Otero et al., 2006).
- The proportion of eggs that develop into larvae (k), which is dimensionless and takes values in the interval $(0, 1)$.
- The proportion of pupae that develop into adult females (f), which is dimensionless and takes values in the interval $(0, 1)$.

Based on these assumptions and parameter definitions, the autonomous dynamical system can be expressed as follows::

$$\begin{cases} \frac{dL}{dt} = kf\phi^*(T)M\left(1 - \frac{L}{C}\right) - (\pi_l^*(T) + \mu_l^*(T))L \\ \frac{dP}{dt} = \pi_l^*(T)L - (\pi_p^*(T) + \mu_p^*(T))P \\ \frac{dM}{dt} = \pi_p^*(T)P - \mu_f^*(T)M \\ L(t_0) = a,\ P(t_0) = b,\ M(t_0) = c \end{cases} \tag{2.2}$$

where all parameters are strictly positive. Based on the previous definitions and descriptions, the resulting diagram of the model is presented in Figure 2.

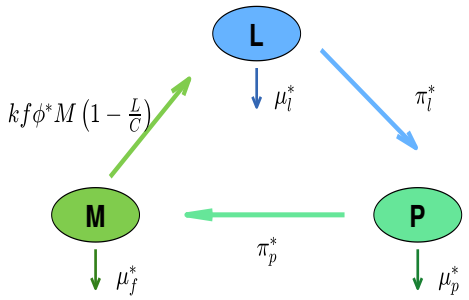

Figure 2: Flow diagram representing the population dynamics of mosquitoes

2.3 Equilibrium and Stability Analysis

2.3.1 Biological Domain

Theorem 2.1. The model (2.2) is biologically and mathematically well-posed in the domain Ω, which is positively forward invariant:

$$\Omega = \left\{ (L,P,M) \in \mathbb{R}^3_+ \mid 0 \le L \le C,\ 0 \le P \le \frac{\pi_l^*(T)}{\pi_p^*(T)+\mu_p^*(T)} \cdot C,\ 0 \le M \le \frac{\pi_p^*(T)}{\mu_f^*(T)} \frac{\pi_l^*(T)}{\pi_p^*(T)+\mu_p^*(T)} \cdot C \right\}$$

Proof. For the system of differential equations (2.2) there exists a unique solution, since the right-hand side is continuous and has continuous partial derivatives in the domain Ω. It is shown that Ω is positively forward invariant. The verification is carried out by analyzing the initial conditions on each boundary of the domain and evaluating the sign of the corresponding derivatives. In all cases, the flow vectors point inward or are null at the boundary, ensuring that no trajectory can leave Ω. Therefore, any solution of system (2.2) with initial conditions in Ω remains in Ω for all $t \ge 0$. □

2.3.2 Equilibrium Points

System (2.2) admits two equilibrium points: the trivial point, representing the absence of mosquitoes,

$$P_0 = \left(\bar{L}_0, \bar{P}_0, \bar{M}_0\right) = (0,0,0) \tag{2.3}$$

and the non-trivial point P_1, representing the presence of mosquitoes conditioned by the specific annual mean temperature T:

$$P_1 = \begin{cases} \bar{L}_1(t) = C\left(1 - \frac{1}{Q_0^*(T)}\right) \\ \bar{P}_1(t) = \frac{\pi_l^*(T)}{\pi_p^*(T)+\mu_p^*(T)} \bar{L} \\ \bar{M}_1(t) = \frac{\pi_p^*(T)}{\mu_f^*(T)} \bar{P} \end{cases} \tag{2.4}$$

The key parameter for the existence of P_1 is the Temperature-Dependent Basic Offspring Number, $Q_0^*(T)$, which represents the average number of viable females produced by a female throughout her lifetime, and is given by:

$$Q_0^*(T) = \frac{\pi_l^*(T)}{\pi_l^*(T)+\mu_l^*(T)} \cdot \frac{\pi_p^*(T)}{\pi_p^*(T)+\mu_p^*(T)} \cdot \frac{kf\phi^*(T)}{\mu_f^*(T)} \quad \text{with } k, f \in (0,1) \tag{2.5}$$

2.3.3 Local Stability

The local stability analysis of the equilibrium points of system (2.2) is performed by evaluating the Jacobian matrix at each equilibrium state and applying the Routh-Hurwitz criterion.

Theorem 2.2. *Let $Q_0^*(T)$ be a given parameter. The following local stability conditions hold:*

1. *If $Q_0^*(T) < 1$, the trivial equilibrium point is locally asymptotically stable.*
2. *If $Q_0^*(T) > 1$, the trivial equilibrium point is unstable.*
3. *If $Q_0^*(T) > 1$, the non-trivial equilibrium point is locally asymptotically stable.*
4. *If $Q_0^*(T) < 1$, the non-trivial equilibrium point is unstable.*

Outline of the proof. The Jacobian matrix of the system is constructed in terms of the transition and mortality rates of each stage. When evaluated at the trivial and non-trivial equilibrium points, a cubic characteristic polynomial is obtained whose coefficients depend on $Q_0^*(T)$. By applying the Routh-Hurwitz criterion, the sign of the real parts of the eigenvalues is determined, which allows establishing the stability conditions as a function of $Q_0^*(T)$.

3 Results and Discussion

3.1 Sensitivity Analysis of $Q_0^*(T)$

The behavior of the mosquito population is intrinsically linked to the value of $Q_0^*(T)$, as established in Theorem 2.2. Therefore, a sensitivity analysis for $Q_0^*(T)$ is performed using the method of normalized local sensitivity coefficients. This method consists of calculating the sensitivity index Γ of each parameter p as:

$$\Gamma_p^{Q_0^*(T)} = \frac{\partial Q_0^*(T)}{\partial p} \frac{p}{Q_0^*(T)} \tag{3.1}$$

An analysis of the partial derivatives of $Q_0^*(T)$ indicates that it is an increasing function of the parameters $\phi^*(T)$, $\pi_l^*(T)$, $\pi_p^*(T)$, k, and f. Conversely, $Q_0^*(T)$ is a decreasing function of the parameters $\mu_l^*(T)$, $\mu_p^*(T)$, and $\mu_f^*(T)$.
The results of the sensitivity index calculations for $Q_0^*(T)$ are presented in Table 2.
According to the magnitude of the indices, the most influential parameters in model (2.2) are $\phi^*(T)$, $\mu_f^*(T)$, k, and f, all with a magnitude of $|1|$. These have a significant impact on the stability of the system, whereas the parameters associated with immature stages ($\mu_l^*(T)$, $\pi_l^*(T)$, $\mu_p^*(T)$, and $\pi_p^*(T)$) exhibit magnitudes lower than $|1|$.
Parameters k, f, and $\phi^*(T)$ show a directly proportional change with respect to $Q_0^*(T)$. For example, if k increases (or decreases) by 30%, $Q_0^*(T)$ also varies by 30%. In contrast, $\mu_f^*(T)$ generates an inversely proportional change in $Q_0^*(T)$.

3.2 Influence of k and f and Simulation Parameters

Keeping k and f constant, $Q_0^*(T)$ follows an increasing curve in the interval $[-15, T_{\max}]$ and a decreasing curve in $[T_{\max}, 45]$, with $T_{\max} \approx 29^\circ$C. The maximum value, $Q_{0\max}^*$, depends on the value of k (Figure 3a) or the value of f (Figure 3b).
Numerical experimentation with the parameters k and f, which are independent of temperature, for different values between 0 and 1, allows the following inferences:

- If $k \to 1$, then $Q_{0\max}^* \to 119$ with $f = 0.6$ (Figure 3a).
- If $k \to 0$, then $Q_{0\max}^* \to 0$ with $f = 0.6$ (Figure 3a).

Table 2: Normalized sensitivity indices for Q_0^*

Parameter	Description	Index (Γ)
$\phi^*(T)$	Per capita oviposition rate at T	$\Gamma_{\phi^*(T)}^{Q_0^*(T)} = 1$
$\mu_l^*(T)$	Larval mortality rate at T	$\Gamma_{\mu_l^*(T)}^{Q_0^*(T)} = -\frac{\mu_l^*(T)}{\pi_l^*(T)+\mu_l^*(T)} \in (-1,0)$
$\pi_l^*(T)$	Transition rate from larva to pupa at T	$\Gamma_{\pi_l^*(T)}^{Q_0^*(T)} = \frac{\mu_l^*(T)}{\pi_l^*(T)+\mu_l^*(T)} \in (0,1)$
$\mu_p^*(T)$	Pupal mortality rate at T	$\Gamma_{\mu_p^*(T)}^{Q_0^*(T)} = -\frac{\mu_p^*(T)}{\pi_p^*(T)+\mu_p^*(T)} \in (-1,0)$
$\pi_p^*(T)$	Transition rate from pupa to adult at T	$\Gamma_{\pi_p^*(T)}^{Q_0^*(T)} = \frac{\mu_p^*(T)}{\pi_p^*(T)+\mu_p^*(T)} \in (0,1)$
$\mu_f^*(T)$	Adult mosquito mortality rate at T	$\Gamma_{\mu_f^*(T)}^{Q_0^*(T)} = -1$
k	Proportion of eggs that develop into larvae	$\Gamma_{k}^{Q_0^*(T)} = 1$
f	Proportion of adult females	$\Gamma_{f}^{Q_0^*(T)} = 1$

- If $f \to 1$, then $Q_{0\,\max}^* \to 179$ with $k = 0.9$ (Figure 3b).
- If $f \to 0$, then $Q_{0\,\max}^* \to 0$ with $k = 0.9$ (Figure 3b).

The results indicate that the parameters k and f can induce extremely high or low values of Q_0^*, regardless of temperature, which in certain scenarios may be biologically unrepresentative.
On the other hand, Figures 3a and 3b show that, when varying the values of k and f, the temperatures at which the threshold $Q_0^*(T) = 1$ is crossed are close to each other and lie approximately within the interval $[14\,^\circ\mathrm{C}, 37\,^\circ\mathrm{C}]$. In this range, $Q_0^*(T) > 1$, and therefore the non-trivial equilibrium P_1 becomes asymptotically stable. Conversely, for temperatures below $14\,^\circ\mathrm{C}$ and above $37\,^\circ\mathrm{C}$ (i.e., within the intervals $[-15\,^\circ\mathrm{C}, 14\,^\circ\mathrm{C})$ and $(37\,^\circ\mathrm{C}, 45\,^\circ\mathrm{C}]$), it holds that $Q_0^*(T) < 1$, and the trivial equilibrium P_0 becomes asymptotically stable.
This behavior, as evidenced in the figures, shows that the persistence of the vector's biological cycle critically depends on the fraction of larvae reaching adulthood k and the proportion of eggs developing into females f. Both parameters determine the threshold-crossing temperatures of $Q_0^*(T) = 1$, and therefore condition the stability of the equilibria P_0 and P_1 as a function of temperature.

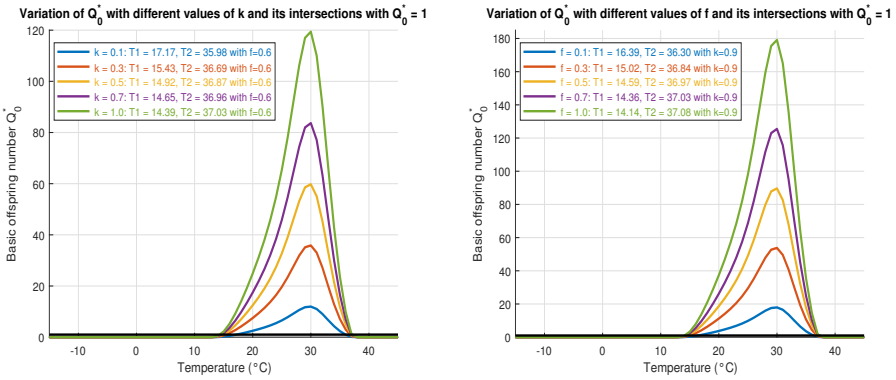

(a) Influence of k on $Q_0^*(T)$ for $0 < k < 1$ (b) Influence of f on $Q_0^*(T)$ for $0 < f < 1$

Figure 3: Influence of k or f on $Q_0^*(T)$ for $T \in [-15, 45]$

For this study, favorable probabilities for mosquito population growth are assumed. Specifically, the temperature-independent parameters k and f are fixed at $k = 0.9$ and $f = 0.6$ across all regions under consideration. This assumption enables the comparison of results among regions with different mean temperatures; however, its principal limitation is that it disregards local ecological variability, which in principle could lead to inconsistencies when extrapolating outcomes to areas with markedly distinct climatic conditions. Nevertheless, in the present analysis no such discrepancies were observed, as the results remained consistent across the regions considered. The rationale for this choice is as follows:

- Parameter k: In departments characterized by tropical or subtropical climates (e.g., Salta), it is reasonable to assume that nearly all *Aedes aegypti* eggs hatch ($k = 0.9$), consistent with Arias et al. (2018). Nevertheless, it is acknowledged that in high-altitude regions such as La Poma this value should be lower. The parameter is kept fixed to facilitate inter-regional comparison.
- Parameter f: The baseline value $f = 0.6$ is adopted, in line with Arias et al. (2018). Values of f approaching zero imply that no female individuals are produced, resulting in a null offspring number at any temperature. Such a scenario precludes the analysis of population variation, as the life cycle is effectively canceled at its inception.

Regarding parameter C, model (2.2) uses it as the carrying capacity, representing the maximum number of individuals that an environment can support, which indeed influences the magnitude of equilibrium populations.
However, the value of C does not alter Q_0^*; consequently, it does not affect the stability of model (2.2). As in Arias et al. (2015), the value of C is normalized to 1. This is not a real biological value or an empirical estimate, but rather a standardization for the analysis of model (2.2), which is maintained throughout the study in order to compare results at different mean temperatures across departments of Salta, Argentina.
Moreover, Couret and Benedict (2014) confirmed that temperature is the most important ecological determinant of the development rate of *Aedes aegypti*. Their meta-analysis demonstrated that temperature alone is sufficient to explain variability in development speed, ranking above other factors such as temperature variability, larval density, diet, and photoperiod. This supports the assumption adopted in the present study of fixing the temperature-independent parameters k and f across regions, while focusing on temperature as the primary driver of mosquito population dynamics.

3.3 Numerical Simulation and Population Dynamics

The numerical solution of system (2.2) was obtained using the *ode45* function in MATLAB, which implements a fourth–fifth order Runge–Kutta method with adaptive time step. Default tolerances were used (relative tolerance 10^{-3} and absolute tolerance 10^{-6}). Initial conditions $L(t_0)$, $P(t_0)$, $M(t_0)$ with $t_0 = 0$ were considered, belonging to the domain Ω, which is positively invariant. The simulation time was set to one year, assigning the following annual mean temperatures T: $22\,^\circ\mathrm{C}$ for Orán, $16\,^\circ\mathrm{C}$ for Capital, and $6.5\,^\circ\mathrm{C}$ for La Poma, corresponding to different departments of the province of Salta.
The values of $Q_0^*(T)$ and the behavior of the solutions for three representative departments (Orán, Capital, La Poma) confirm the prediction of the stability analysis in Theorem 2.2:

- When $Q_0^*(T) > 1$ (Orán and Capital), the solution converges to the non-trivial equilibrium state (P_1) as $t \to \infty$, indicating processes of (re)colonization (see Figures 4a and 4b).
- When $Q_0^*(T) < 1$ (La Poma), the solution converges to the trivial equilibrium state (P_0), reflecting the long-term absence of mosquitoes (see Figure 4c).

Chanampa et al. (2019), based on their field results, reported the presence of *Aedes aegypti* in different localities of the province of Salta, with greater abundance in warmer areas such as Orán and lower abundance in colder regions such as La Poma. In contrast, the mathematical model predicts vector persistence only when $Q_0^*(T) > 1$, which corresponds to the stable non-trivial equilibrium. Thus, the observed presence in Orán provides empirical evidence consistent with the theoretical persistence

predicted by the model, while the absence in La Poma reflects the extinction predicted by the trivial equilibrium ($Q_0^*(T) < 1$). This distinction provides a clear link between field data and mathematical predictions, reinforcing the validity of the approach.

Abán et al. (2022) noted that the study focuses on Orán as an area where field data confirm that the mosquito *Aedes aegypti* maintains an active, widespread, and persistent presence in the city. In this sense, the larger magnitude of $Q_0^*(T)$ in Orán (34.148), compared to Capital (4.6774), reflects a significantly higher level of population persistence at the non-trivial equilibrium, as shown in Figures 4a and 4b, in agreement with empirical evidence. Thus, the elevated value of $Q_0^*(T)$ in Orán is consistent with the sustained presence of *Aedes aegypti* reported by Abán et al., while Chanampa et al. indicate that in Capital the presence of the vector is lower, which corresponds to the reduced value of $Q_0^*(T)$.

Furthermore, Gutierrez et al. (2022) concluded that mosquito abundance is closely linked to climate and urban structure, with meteorological variability, especially rainfall, temperature, and relative humidity, emerging as the primary driver of vector dynamics. These findings underpin the ecological rationale of the present modeling approach, particularly the emphasis on temperature as the dominant factor in mosquito population dynamics.

Unlike Yang et al. (2009, 2011), who fitted entomological parameters using polynomials in the range $10°\text{C} - 40°\text{C}$, and Otero et al. (2006), who employed the Schoolfield equation to describe functional dependence on temperature, this work proposes a piecewise redefinition of the parameters. This strategy ensures mathematical continuity and avoids inconsistencies outside experimental intervals, allowing the analysis to be extended to extreme temperature scenarios such as those observed in La Poma. In this way, the validity of equilibrium and stability conclusions is preserved, and the applicability of the model in local contexts is reinforced.

Finally, Lana et al. (2022) analyzed the abundance of *Aedes aegypti*, illustrating how it is measured through ovitraps and sticky traps, and how factors such as rainfall and temperature generate population peaks with marked spatial heterogeneity in urban areas. Similarly, Estallo et al. (2015) developed a forecasting model in Orán, Argentina, demonstrating that minimum temperature and rainfall are critical drivers of oviposition dynamics, and concluding that such a model can serve as an early warning tool for public health authorities. In contrast, the simulations presented here do not aim to reproduce population patterns or provide short-term forecasts, but rather to capture conditions of persistence and stability under different temperature scenarios, thereby focusing the scope of the model on ecological persistence rather than local fluctuations in abundance. In this context, ecological persistence is understood as the capacity of an *Aedes aegypti* population to survive and remain stable within an environment over time, beyond short-term variations in density.

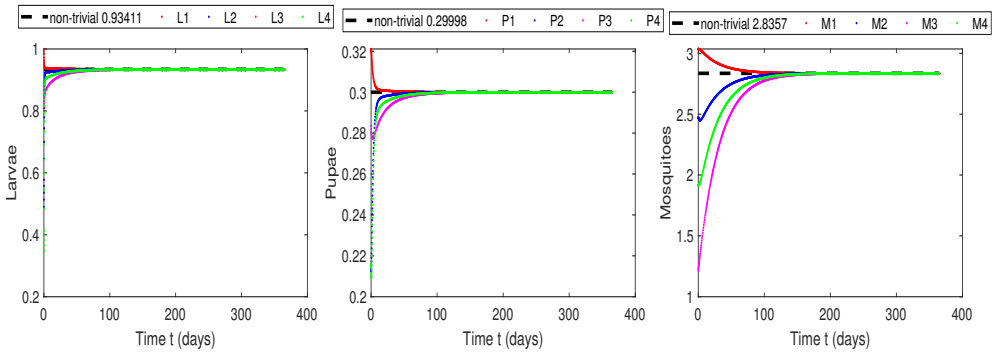

(a) Orán ($T = 22\,^{\circ}\mathrm{C}$)

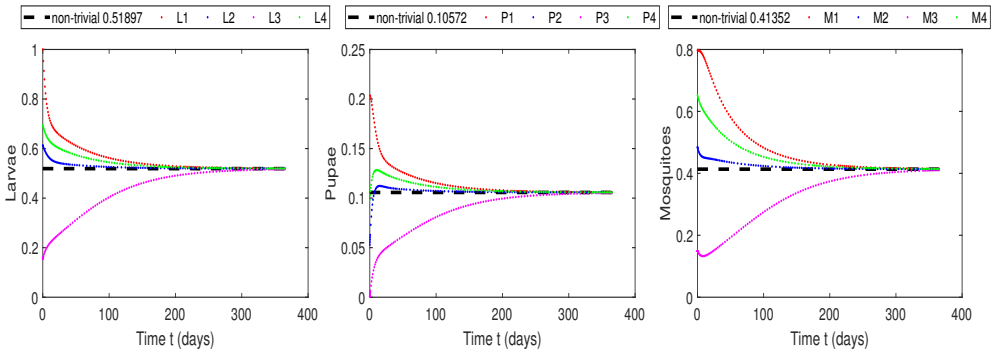

(b) Capital ($T = 16\,^{\circ}\mathrm{C}$)

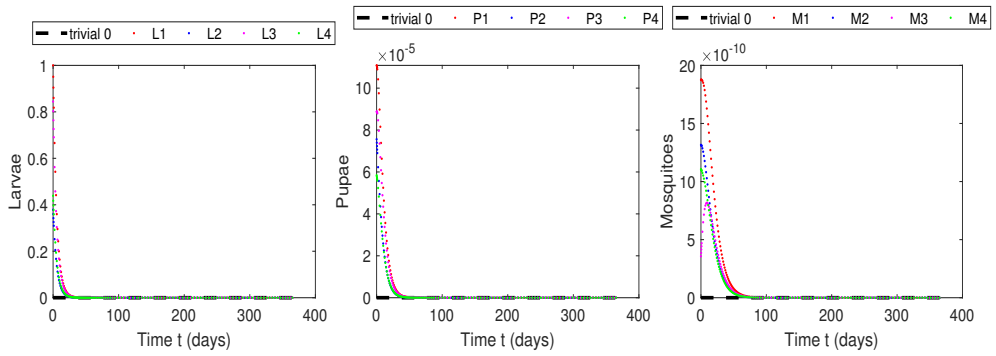

(c) La Poma ($T = 6.5\,^{\circ}\mathrm{C}$)

Figure 4: Numerical simulations of the population dynamics of *Aedes aegypti* in three departments of Salta.

3.4 Bifurcation

The stability is summarized in Figure 5, where the vertical axis represents the first component of the equilibrium points and the horizontal axis corresponds to the bifurcation parameter $Q_0^*(T)$. For the

construction of the curve $\bar{L}_0$, Equation (2.3) is employed, while for the curve $\bar{L}_1$, Equation (2.4) is used, considering $Q_0^*(T)$ as the variable and keeping k, f, and C constant.
The equilibrium $\bar{L}_1$ always exists mathematically, since by definition $Q_0^*(T)$ is positive; however, it is biologically valid only if $Q_0^*(T) > 1$. Thus, when $Q_0^*(T) < 1$, the trivial equilibrium $\bar{L}_0$ is asymptotically stable; whereas, once the threshold $Q_0^* = 1$ is crossed, $\bar{L}_1$ becomes asymptotically stable and $\bar{L}_0$ loses stability.
Consequently, the bifurcation is transcritical: at the critical point the equilibria persist but exchange stability.

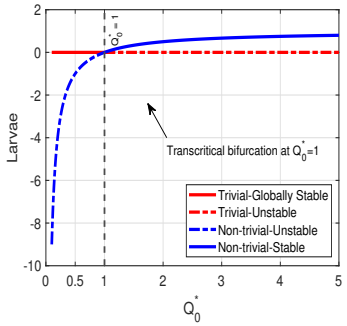

Figure 5: Bifurcation Diagram

4 CONCLUSIONS

a In Section (1), the epidemiological context and the dengue problem in the province of Salta were presented, highlighting the relevance of a mathematical approach for its study. Existing knowledge and previous mathematical models related to dengue transmission and the dynamics of its vector, *A. aegypti*, were reviewed. Based on this introduction, the objectives guiding the present research were formally established, together with the working hypothesis.

b In Section (2), the population model of *Aedes aegypti*, along with its equilibrium points and stability conditions, was originally proposed by Yang et al. for entomological parameters defined in the range of 10 to $40\,^{\circ}\mathrm{C}$. In this work, that temperature range was extended through a piecewise redefinition of the entomological parameters, ensuring mathematical continuity and consistency. It was verified that the equilibrium and stability conclusions obtained by Yang remain valid under this extension, and it was additionally demonstrated that the biological domain, now explicitly conditioned by temperature, is positively invariant. In summary, with this modification in the definition of entomological parameters, the system preserves its mathematical and ecological validity.

c In Section (3), the analysis confirms that the population dynamics of *Aedes aegypti* are strongly conditioned by temperature through $Q_0^*(T)$, with the parameters $\phi^*(T)$, k, f, and $\mu_f^*(T)$ being the most determinant. The simulations show that the model reproduces local patterns of persistence in warmer regions (Orán, Capital) and extinction in colder regions (La Poma), thereby verifying the theoretical predictions and ensuring the biological coherence of the approach. Furthermore, the presence of a *transcritical bifurcation* is observed at the threshold $Q_0^*(T) = 1$, where stability shifts from the trivial equilibrium (P_0) to the non-trivial equilibrium (P_1). This result confirms that the persistence or extinction of the vector depends critically on the annual mean temperature, reinforcing the biological interpretation of the model.

References

1. Dirección Nacional de Epidemiología y Análisis de Situación de Salud. (2021). Ministerio de Salud de la Nación: Boletín Integrado de Vigilancia, (296, 335, 447, 479, 410, 613, 561).

2. Avilés, G., Rangeon, G., Baroni, P., Paz, V., Monteros, M., Enria, D., & Sartini, J. L. (2000). Epidemia por virus dengue-2 en Salta, Argentina, 1998.

3. Chanampa, M. M., Gleiser, R., & Aparicio, J. P. (2019). Distribución y abundancia de Aedes aegypti en la provincia de Salta: asociación con factores ambientales.

4. Dirección General de Coordinación Epidemiológica. (2023). Boletín Epidemiológico - Provincia de Salta, Argentina. http://saladesituacion.salta.gov.ar/web/inicio/boletines/documentos/boletin _ 132023.pdf

5. Yang, H. M., Macoris, M. L. D. G., Galvani, K. C., Andrighetti, M. T. M., & Wanderley, D. M. V. (2009). Assessing the effects of temperature on the population of Aedes aegypti, the vector of dengue. Epidemiology and Infection, 137(8), 1188–1202. https://doi.org/10.1017/S0950268808001907

6. Yang, H. M., Boldrini, J. L., Fassoni, A. C., Freitas, L. F., Gomez, M. C., de Lima, K. K., & de Oliveira, F. T. M. (2011). Aedes aegypti population dynamics: Model comparison. Ecological Modelling, 222(19), 3601–3611. https://doi.org/10.1016/j.ecolmodel.2011.07.013

7. Bar-Zeev, M. (1958). The effect of temperature on the growth rate and survival of the immature stages of Aedes aegypti (L.). Bulletin of Entomological Research, 49(1), 157–163. https://doi.org/10.1017/S0007485300052893

8. Focks, D. A., Haile, D. G., Daniels, E., & Mount, G. A. (1993). Dynamic life table model for Aedes aegypti (Diptera: Culicidae): analysis of the literature and model development. Journal of medical entomology, 30(6), 1003-1017.

9. Alonso, L. E., Romeo Aznar, V., & Solari, H. G. (2022). Why Is Aedes aegypti Moving South in South America? Mathematics, 10(23), 4510. https://doi.org/10.3390/math10234510

10. San Miguel, T. V., Da Re, D., & Andreo, V. (2024). A systematic review of Aedes aegypti population dynamics models based on differential equations. Acta Tropica, 260, 107459. https://doi.org/10.1016/j.actatropica.2024.107459

11. Eiman, M., et al. (2010). Directrices para el control de vectores. Organización Mundial de la Salud.

12. Otero, M., Solari, H. G., & Schweigmann, N. (2006). A stochastic population dynamics model for Aedes aegypti: Mathematical analysis and validation. Ecological Modelling, 198(3–4), 316–332. https://doi.org/10.1016/j.ecolmodel.2006.05.011

13. Arias, J. H., Martínez, H. J., Sepúlveda, L. S., & Vasilieva, O. (2018). Estimación de los parámetros de dos modelos para la dinámica del dengue y su vector en Cali, Colombia. Ingeniería y Ciencia, 14(28), 69–92.

14. Arias, J. H., Martinez, H. J., Sepulveda, L. S., & Vasilieva, O. (2015). Predator-prey model for analysis of Aedes aegypti population dynamics in Cali, Colombia. International Journal of Pure and Applied Mathematics, 105(4), 561–597.

15. Couret, J. & Benedict, M. Q. (2014). A meta-analysis of the factors influencing development rate variation in Aedes aegypti (Diptera: Culicidae). BMC ecology, 14, 3. https://doi.org/10.1186/1472-

6785-14-3

16. Abán Moreyra, D. N., Castillo, P. M., Escalada, A., Mangudo, C., Copa, G. N., Gleiser, R. M., Nasser, J. R., & Gil, J. F. (2022). Use of Aedes aegypti oviposition surveillance and a geographic information system for planning antivectorial measures. The American Journal of Tropical Medicine and Hygiene, 107(4), 916–924. https://doi.org/10.4269/ajtmh.21-0364

17. Gutierrez, J. A., Laneri, K., Aparicio, J. P., & Sibona, G. J. (2022). Meteorological indicators of dengue epidemics in non-endemic Northwest Argentina. Infectious Disease Modelling, 7(4), 823–834. https://doi.org/10.1016/j.idm.2022.10.004

18. Lana, R. M., Carneiro, T. G., Honório, N. A., & Codeço, C. T. (2011). Multiscale analysis and modelling of Aedes aegyti population spatial dynamics. Journal of Information and Data Management, 2(2), 211-211.

19. Estallo, E. L., Ludueña-Almeida, F. F., Introini, M. V., Zaidenberg, M., & Almirón, W. R. (2015). Weather variability associated with Aedes (Stegomyia) aegypti (Dengue vector) oviposition dynamics in Northwestern Argentina. PLoS One, 10(5), e0127820.